Proceedings of ASME Turbo Expo 2011
GT2011
June 6-10, 2011, Vancouver, British Columbia, Canada

GT2011-45166

RESEARCH OF DESIGN METHOD OF VARIABLE AREA NOZZLE TURBINE FOR VARIABLE CYCLE ENGINE

YIN Zhao[1], FANG Xiang-jun[1], LIU Si-yong[1], WANG Ping[1], LIU Zhi-gang[2]
1 Beihang University, Beijing 100191, P. R. China
2 Civil Aviation University of China, Tianjin 300300, P. R. China
E-mail: yinzhao-2008@163.com

ABSTRACT

One stage of Variable Area Nozzle Turbine (VANT) was designed for a Variable Cycle Engine (VCE) as the low pressure stage. The design method is presented in this article, where one of the objective conditions of the turbine is chosen as design condition while other objective conditions are simulated by CFD tools to verify its performance. The turbine profiles were designed with a three-dimensional (3D) profile design method based on S_1 stream surfaces according to the chosen condition.

Steady numerical simulations were used to acquire a series of turbine characteristic maps under many operating conditions with different vane stagger angles, and as anticipated, the turbine has reached high efficiency and met both the flow rate and expansion ratio demands under at least two objective conditions, which verifies that the design method is feasible and successful, however performance differences were found between the two objective conditions.

In order to analyze deeply the differences, steady and unsteady flows of the turbine in both objective conditions were also simulated. Based on the blades pressure distribution, total pressure loss distribution, velocity distribution and wake transport, the results revealed the causes of low efficiency under off-design condition and different unsteady fluctuations between two objective conditions, which provides more reference for the design method of VCE turbine in the future.

INTRODUCTION

Variable cycle engine can obtain excellent thermodynamic cycle performances under different operating conditions by adjusting its components to broaden the flight envelops of aircraft and enable the aircraft to cruise under supersonic and subsonic conditions with low Specific Fuel Consumption (SFC), which represents the future trend of aeroengine [1-3]. The variable components include variable geometry fan, variable geometry high pressure compressor, variable geometry turbine, variable area nozzle and so on. Variable geometry turbine is able to adjust flow rate and expansion ratio by changing the vane throat area, which is achieved through the alteration of the vane stagger angle in this article.

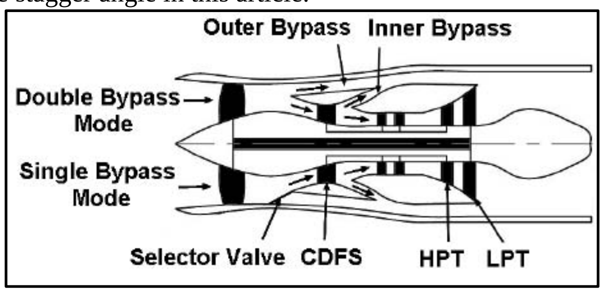

Figure 1. Work mode of VCE discussed in this article

The work mode of VCE discussed in this article is presented in Fig.1 [4]:

Single Bypass Mode: The selector valve is closed and all air goes through the Core Drive Fan Stage (CDFS). The fan bypass flow bypasses the core engine through the inner bypass duct and remixes with the core flow downstream of the low pressure turbine. The nozzle is full open to shift the loading to the HP shaft to cope with the added work of the CDFS. At the same time, the expansion ratio and the flow rate rise to increase the specific thrust with low bypass ratio under supersonic and acceleration condition.

Double Bypass Mode: The selector valve is full open and the nozzle is now closed to unload the HP turbine and load the LP turbine. The bypass ratio increases for best specific fuel consumption for subsonic cruise and best exhaust velocity conditions for improved noise suppression on takeoff.

No matter in the single bypass mode or the double bypass mode, the turbine must adapt itself to the changes of compressor's conditions and guarantee good performance of the engine. Therefore, when the engine switches its work modes, the compressor also changes its conditions, and the turbine must adapt to the alterations which means that the turbine must keep high efficiency even if it works in greatly different conditions, which we call as the objective conditions in order to match the compressor.

Turbine, as a core component, its parameters, such as inlet pressure and temperature, flow rate and expansion ratio, will be changed greatly so that their off-design conditions are out of the ranges of traditional turbine characteristic maps when the VCE's thermodynamic cycle parameters vary, meanwhile the turbine needs to maintain high efficiency. Therefore, compared with the conventional turbine where only one operating condition needs to be considered, the VCE turbine has to satisfy the demands of several operating conditions, which must be considered when it is designed.

In this article, firstly the design condition was chosen from a series of objective conditions which match with different compressor conditions when VCE switches its work modes. Then the turbine was designed by a 3D profile design method based on S_1 stream surface [5,6] according to the chosen design condition. In order to verify its flow rate, expansion ratio, especially its stagnation efficiency and capacity, other objective conditions of the turbine were also simulated by CFD tools after the vane was rotated to predicted stagger angles.

Two objective conditions were provided presently in high bypass ratio mode and low bypass ratio mode respectively. Correspondingly, two characteristic maps were acquired by solving the steady Reynolds average Navier-Stokes equations to evaluate the performance of the turbine with two different stagger angles. And specific steady flows in the turbine were analyzed to find the reasons that cause low efficiency in off-design condition.

Considering the effects of the potential flow, the transmission of wake and the development of vortex, the real flows are unsteady [7,8]. The excitation force caused by the unsteady flows will lead to low efficiency and high-cycle fatigue. So the unsteady features are also discussed in this article. The unsteady flows in the turbine were simulated using Domain Scaling Method [9] to reveal the causes of different unsteady fluctuations between two objective conditions.

DESIGN METHOD

Different from the conventional turbine which is designed under one certain operation condition, the VANT has to satisfy aerodynamic aims under a series of working conditions, and it's different from other components of VCE such as the high pressure turbine [10] because its geometry also varies.

Assuming that the VCE works in *m* conditions, the turbine must correspond with *m* series of parameters as follows:

Condition *1*	$P^*_{in,1}$	$T^*_{in,1}$	G_1	μ_1	n_1	$\pi^*_{T,1}$	$\geq \eta^*_{T,1}$
Condition *2*	$P^*_{in,2}$	$T^*_{in,2}$	G_2	μ_2	n_2	$\pi^*_{T,2}$	$\geq \eta^*_{T,2}$
……		……					
Condition *i*	$P^*_{in,i}$	$T^*_{in,i}$	G_i	μ_i	n_i	$\pi^*_{T,i}$	$\geq \eta^*_{T,i}$
……		……					
Condition *m*	$P^*_{in,m}$	$T^*_{in,m}$	G_m	μ_m	n_m	$\pi^*_{T,m}$	$\geq \eta^*_{T,m}$

These objective conditions of turbine come from different modes of VCE, which makes the turbine match with the characteristic maps of the compressor. Obviously it is very difficult to design the turbine to meet so many series of cycle parameters.

For turbomachinery, the total-total efficiency is commonly depended on ten parameters, namely,

$$\eta^*_T = (P^*_{in}, T^*_{in}, \pi^*_T, G, R, k, \mu, n, D, L) \quad (1)$$

The geometry and gas parameters can be omitted for the same turbine and the same working fluid. The following equations can be gotten from the similarity principle in turbomachinery.

$$\eta^*_T = (\pi_1, \pi_2, \pi_3, \pi_4, \pi_5) \quad (2)$$

Where, expansion ratio $\quad \pi_1 = \pi^*_T = P^*_{in}/P^*_{out} \quad (3)$

Reduced mass flow rate $\quad \pi_2 = \overline{G} = G\sqrt{T^*_{in}}/P^*_{in} \quad (4)$

Reynolds No. $\quad \pi_3 = P^*_{in}/\mu\sqrt{T^*_{in}} \quad (5)$

Reduced power $\quad \pi_4 = \overline{L} = L/P^*_{in}\sqrt{T^*_{in}} \quad (6)$

Reduced speed $\quad \pi_5 = \overline{n} = n/\sqrt{T^*_{in}} \quad (7)$

Both π_1 and π_4 are the qualitative parameters and can be represented into:

$$\pi_1 = \pi^*_T = f_1(\pi_2, \pi_3, \pi_5) \quad (8)$$

$$\pi_4 = \overline{L} = f_2(\pi_2, \pi_3, \pi_5) \quad (9)$$

Thus, the efficiency is also represented into:

$$\eta^*_T = f_3(\pi_2, \pi_3, \pi_5) \quad (10)$$

The effect of π_3 can be ignored if Re is bigger than the second critical Reynolds number in turbomachinery. Equation 10 is reduced as:

$$\eta^*_T = f_3(\pi_2, \pi_5) = f_3\left(G\sqrt{T^*_{in}}/P^*_{in}, n/\sqrt{T^*_{in}}\right) = f_3(\overline{G}, \overline{n}) \quad (11)$$

Therefore, if we make following equations both 12 and 13 to be established for turbine of VCE, the multi-conditions turbine for VCE can be treated as the conventional turbine to be designed.

$$\overline{G} = G_1\sqrt{T^*_{in,1}}/P^*_{in,1} = G_i\sqrt{T^*_{in,i}}/P^*_{in,i} \quad (i = 1,2,\cdots,m) \quad (12)$$

$$\overline{n} = n_1/\sqrt{T^*_{in,1}} = n_i/\sqrt{T^*_{in,i}} \quad (i = 1,2,\cdots,m) \quad (13)$$

But, it's very difficult to make equations both 12 and 13 to be established and make all reduced mass flow values equivalent in all kinds of conditions. So the designer has to face the conditions as follows:

$$G_1\sqrt{T^*_{in,1}}/P^*_{in,1} \neq G_2\sqrt{T^*_{in,2}}/P^*_{in,2} \neq \cdots \neq G_i\sqrt{T^*_{in,i}}/P^*_{in,i} \quad (i = 3,\cdots,m) \quad (14)$$

$$n_1/\sqrt{T^*_{in,1}} \neq n_2/\sqrt{T^*_{in,2}} \neq \cdots \neq n_i/\sqrt{T^*_{in,i}} \quad (i = 3,\cdots,m) \quad (15)$$

The designer can change the stagger angle of vane to adjust the mass flow because the reduced mass flow is depended on the throat of nozzle. Therefore we choose one condition as the design condition such as condition i and the other objective conditions are regarded as the conditions to be examined. If the designed turbine is able to reach the demands of flow rate, power and so on by adjusting the stagger angle of its nozzle, meanwhile the efficiencies are not lower than the aim values, then we think it is successful for the turbine to be designed.

As an example, two objective conditions were provided presently in high bypass ratio mode and low bypass ratio mode respectively, and the latter one with bigger stagger angle was chosen as the design condition, while the performance under another conditions needs to be examined to verify the feasibility of the method. The profiles of the blades at mid-span in two modes are shown below (Fig.2).

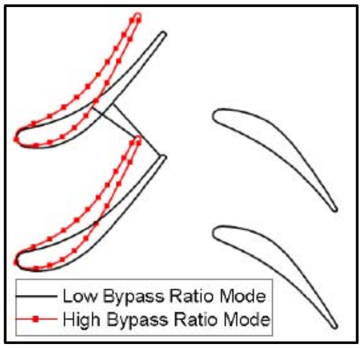

Figure 2. Profiles of stator and rotor at mid-span in two modes

The conventional cylindrical modeling method transforms the throughflow results with 3D features onto two-dimensional (2D) plane, which will cause inevitably design error especially with large expansile meridional channel and sophisticated streamlines. So a blade design method based on S_1 stream surface which corresponds to the streamline calculated in throughflow results is performed for the design condition (Fig.3).

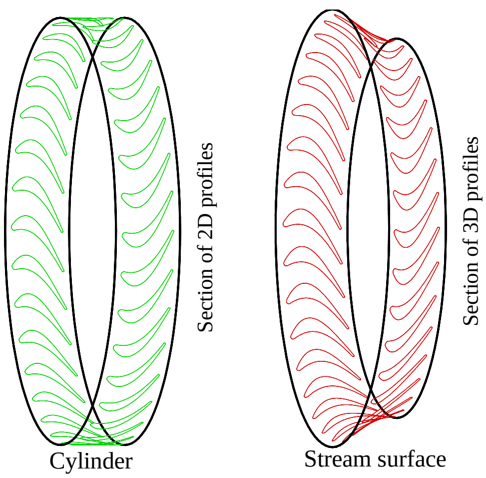

Figure 3. 3D profiles defined in general surface of revolution

A mapping relationship between the 3D S_1 surface and a new 2D surface is established through this method firstly, based on the premise of the same length of streamline and same flow angle between the two spaces, so as to apply the classical 2D design method on profile modeling. Then the finished 2D profile is mapped back to the 3D S_1 stream surface. A series of profiles can be acquired in this way and the 3D blade will be formed as they are stacked together.

CHARACTERISTIC MAPS IN TWO DIFFERENT BYPASS RATIO MODES

Computation Method

FINE/Autogrid was employed to generate multi-block structured grids for the turbines in low bypass ratio mode (Fig.4) and high bypass ratio mode. Each row was divided into five blocks, one of which was O-type around the blade and others were H-type. To assure the calculating precision, near-wall grid was refined and y+ calculated around the blades was verified less than 10 to satisfy the demand of the solver.

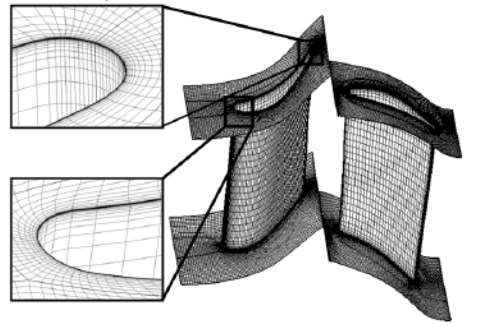

Figure 4. CFD mesh in high bypass ratio mode

The flows of turbine under different operating conditions were simulated by solving the steady Reynolds averaged N-S equation using S-A one equation model. Fine/Turbo is employed to simulate the flows in the turbines. Central difference scheme is applied in space, and local time step and multi-grid technique are used to accelerate convergence. Total pressure and total temperature at inlet and static pressure at outlet are given as boundary conditions.

Characteristic maps of the turbine under four reduced speeds of 0.9, 0.95, 1.0 and 1.05 are calculated in two modes with different bypass ratios.

Analysis of Characteristic Maps in Two Modes

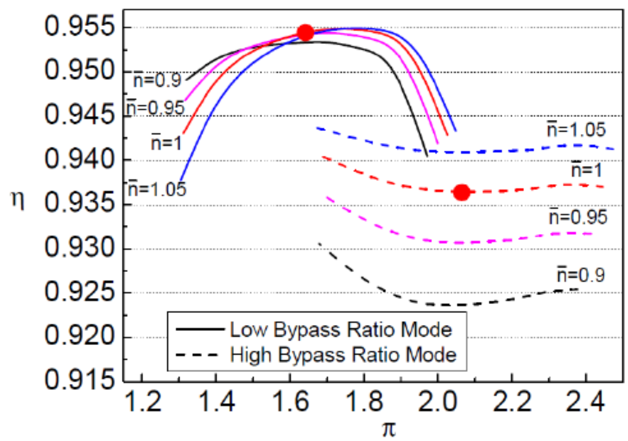

Figure 5. Efficiency characteristic maps

The dots in Fig.5 represent the performances of the turbine under two objective conditions. On the whole, the efficiency of turbine in low bypass mode is greater than that in high bypass ratio mode. The efficiency in low bypass mode varies less with relative speed, while it is sensitive to the change of expansion ratio. But in high bypass ratio mode, the efficiency variation is higher with different reduced speed at the same expansion ratio, which makes significant difference between two modes when the reduced speed decreases. And the efficiency curves are more gentle in high bypass ratio mode.

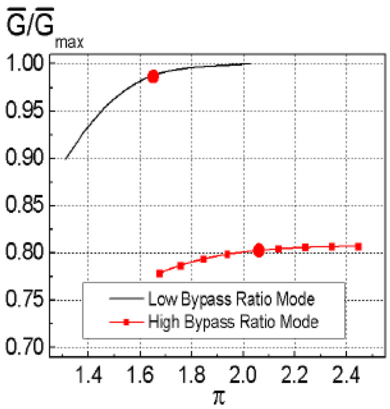

Figure 6. Mass flow characteristics.

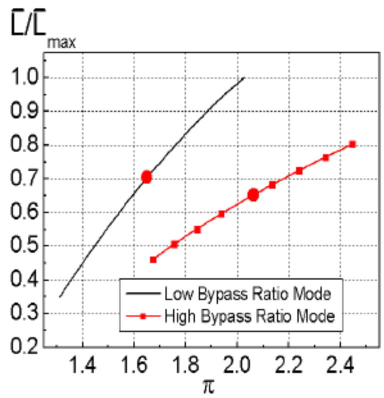

Figure 7. Power characteristics

The variation of flow characteristics and power characteristics with reduced speed is not significant, so two kinds of characteristic lines of mass flow and power in two objective conditions at the reduced speed of 1 are shown in Fig. 6 and Fig. 7 respectively.

The mass flow curves were normalized to the choked reduced flow of the turbine in low bypass ratio mode. The reduced flow rates in two objective conditions increase to the choking flow limited by the throat area with the increase of expansion ratio, while the growth slows down. The reduced flow rate drops 18.8% as the stagger angle decreases 10 degrees, which shows that it's effective to adjust the flow rate by changing the stagger angle.

The power curves were normalized to the maximum value in low bypass ratio mode. The values in two objective conditions increase almost linearly with the increase of expansion ratio, while the gradient in low bypass ratio mode is greater with stronger flow capacity. The reduced power decreases 8.25% as the stagger angle decreases 10 degrees.

From the results above, it's verified that the efficiency, flow capacity and power capacity in two modes with different stagger angles have reached the goal without choking. Specific reasons for the different efficiencies will be discussed in the followings chapters.

ANALYSIS OF STEADY FLOWS

Simulations of steady flows on two conditions are presented here.

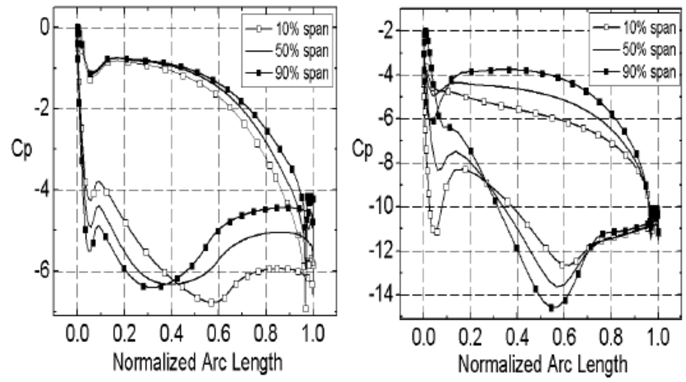

(a) stator (b) rotor

Figure 8. Pressure distributions in low bypass ratio mode

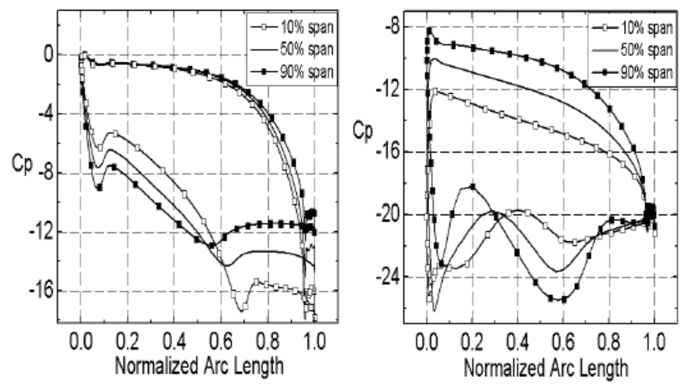

(a) stator (b) rotor

Figure 9. Pressure distributions in high bypass ratio mode

Distributions of static pressure at different spanwise positions of stator and rotor in two modes are shown in Fig. 8 and Fig. 9 respectively. The pressure coefficient (Cp) is defined as follows:

$$Cp = (P - P_{in}^{*})/(\rho_{in} u_{in}^{2}/2) \quad (16)$$

The pressure distributions of stator on the pressure side vary slightly. On the suction side, the flows start expansion dramatically at the position of 5% axial chord and then accelerate slowly to the lowest pressure point in two modes. The axial position of the end of expansion varies between the two modes. The stagger angle turns smaller in the high bypass ratio mode, which makes the change of curvature at leading edge more gentle to extend the expansion region. And as the reaction decreases, the pressure in the stator drops more with little deceleration occurring on the suction side which is desirable. As shown in the pressure distribution, the radial pressure differential is greater in diffusion of the high bypass ratio mode, and it causes obvious radial secondary flows which can be seen later in the distribution of total pressure loss at stator outlet. The low energy flows within the boundary layer move to the hub under the action of radial secondary flows to cause more loss.

From the pressure distributions on the suction sides of rotor, it can be seen that in the high bypass ratio mode the pressure decreases to minimum around the leading edge, which is even lower than the end the expansion. The adverse pressure gradient is so great that separation is likely to occur. And the stagnation point moves closer to the leading edge with the growth of radius because of different income flow angle along the radial direction. The shapes of the rotor's pressure differ a lot in the two modes, and specific reasons will be discussed later.

Total pressure loss at stator outlet in two modes is presented here to analyze the wake and secondary flow losses. The total pressure loss coefficient (ξ) is defined as follows:

$$\xi = (P^* - P_{in}^*)/P_{in}^* \tag{17}$$

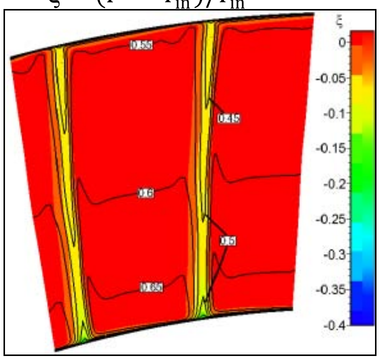

(a) Low bypass ratio mode

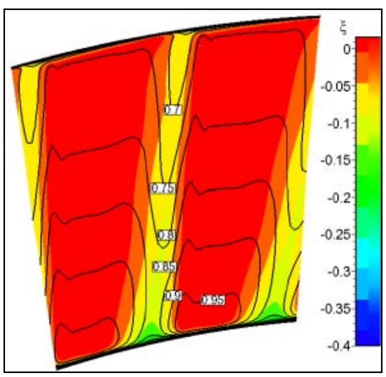

(b) High bypass ratio mode

Figure 10. Total pressure loss contours and isoline of Mach number at stator outlet

The total pressure loss at stator outlet in high bypass ratio mode is higher as shown in Fig.10, and the absolute value increases 1.25% compared to low bypass ratio mode. On one hand, the pressure differential between suction side and pressure side shown in Fig.9 is higher to cause more wake loss. On the other hand, the radial secondary flows are stronger in the boundary layer of suction side which causes the low energy flows to pile up around the hub. At the same time, the shape of wake along the radius in high bypass ratio mode is not as straight as it is in low bypass ratio mode. The wake shifts towards the suction side at the tip under the action of increasing pressure differential between pressure side and suction side along the radial direction, and causes uneven distribution of exit angle along radius at the stator outlet shown in Fig.11. The distribution of Mach number at the outlet in low bypass ratio mode is more uniform with lower gradient in the wake region which is consistent with the distribution of radial secondary flows.

As shown in Fig.11, the stagger angle plays an important role in the exit angle to influence the attack angle of rotor downstream.

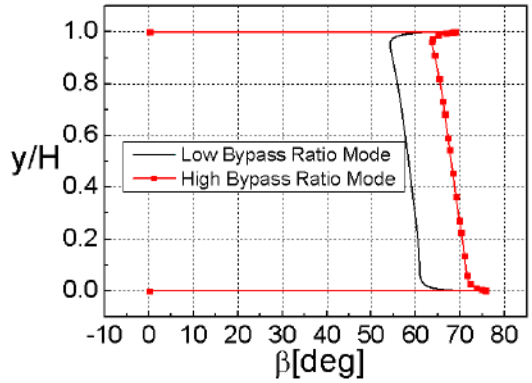

Figure 11. Distribution of exit angle at stator outlet in two modes

The flow fields on S_1 stream surface of the rotor in two modes are shown in Fig. 12, and the black points represent the stagnation points. It's clear that different attack angles and boundary conditions cause different cascade losses in two modes.

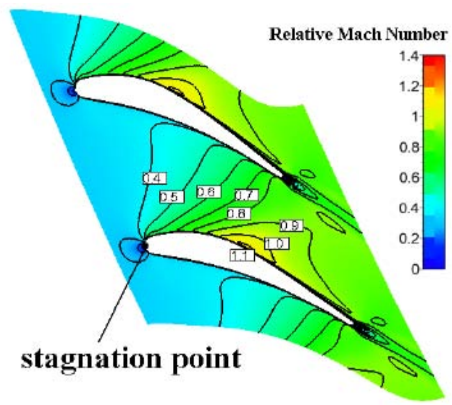

(a) Low bypass ratio mode

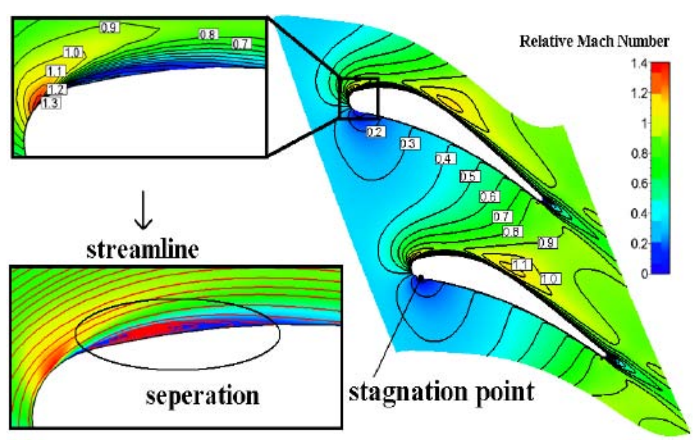

(b) High bypass ratio mode

Figure 12. Distribution of relative Mach number and streamline at 50% span in the rotor of two modes

In high bypass ratio mode, the stagnation point almost divorces from the leading edge and the flow beats on the pressure side directly. The flow above the stagnation point has to bypass the leading edge to the suction side which causes strong secondary flows, while it is compressed violently to generate shock wave in local area. In the shock region, the suddenly increased pressure makes the boundary layer thicker. This shock-boundary interaction leads to separation after the shock region inevitably, and the separation lasts for about 13% axial chord. The length of adverse pressure in the diffuser is much longer than the low bypass ratio mode shown in Fig.8 and Fig. 9. But in low bypass ratio model, separation doesn't appear and the maximum Mach number is 1.2 which is much lower.

Considering the stronger 3D effect of the stator in high bypass ratio mode and the fact that the hub is more critical from the standpoint point of rotor reaction, the flows near the hub and shroud are also presented. The results show that separation at the hub is more severe with stronger shock and the separation lasts about 20% axial chord. It also can be found that a long adverse pressure section exits in the main stream after expansion. Meanwhile the flows at the shroud with appropriate attack angle perform better without any separation. So it can be referred that the decreased reaction and large attack angle play an important role in the low efficiency of the turbine in high bypass ratio mode.

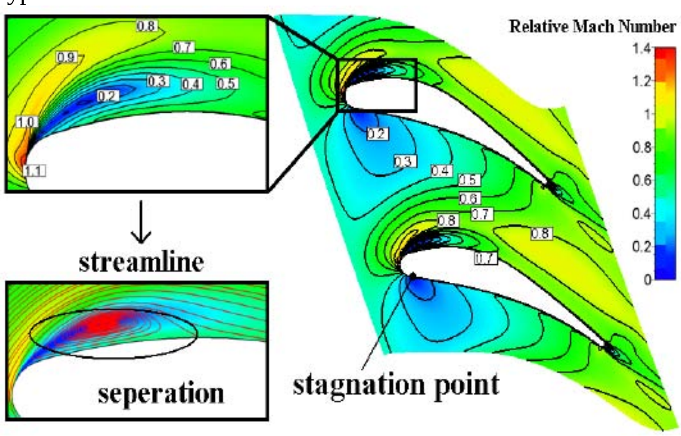

(a) 10% Span

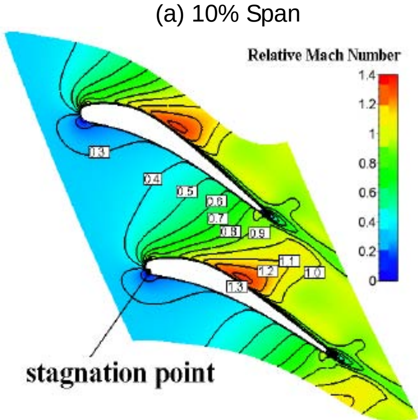

(b) 90% Span

Figure 13. Distribution of relative Mach number and streamline in the rotor of high bypass ratio mode

ANALYSIS OF 3D UNSTEADY FLOWS

Computation Method

Presently, Domain Scaling Method is used to deal with the unsteady rotor/stator interface based on the constraint that the pitch distance must be identical on both sides of the interface. But the turbine's stator and rotor have different numbers, 55 and 56 respectively, which means that the geometry has to be scaled firstly. In order to reduce the influence of scaling on the computation accuracy, the stator was scaled and the number was changed to 56 on condition that the pitch chord ratio should keep unchanged [11]. The trailing edge point was chosen as the reference point to reduce the effect of the rotor/stator spacing on flows.

The grids generation adopts the same topology used in the steady simulation. Dual time step approach [12] is implemented for time marching in computation. The time used for a rotor crossing one stator passage is called one period which is divided into 40 physical time steps. 100 iterations are calculated in pseudo time domain for each physical time step. The relative errors between the average flow rate of unsteady simulation results and steady simulation results in both modes are less than 0.2% verifying that the scaling method is reasonable.

Analysis of Unsteady Simulation Results

The pressure disturbance of suction side of rotor and exit angle disturbance at stator outlet in two modes are presented in Fig.14 and Fig.15 to compare the unsteady phenomenon, and the coefficients are defined as follows:

$$\widetilde{P} = \frac{1}{\overline{P}}\sqrt{\frac{1}{40}\sum_{i=1}^{40}(P_i - \overline{P})^2} \tag{18}$$

$$\tilde{\beta} = (\beta_i - \overline{\beta})/\overline{\beta} \tag{19}$$

The pressure disturbance of the rotor is more intense in high bypass ratio mode as shown in Fig.14 accompanied with shock wave and separation, especially in the leading edge. In contrary, the exit angle disturbance at stator outlet is lower in high bypass ratio indicating that the potential flow is not the determinant factor of pressure fluctuation.

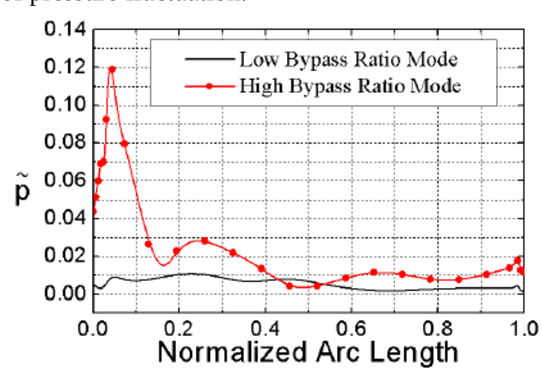

Figure 14. Pressure disturbance of suction side of rotor in two modes

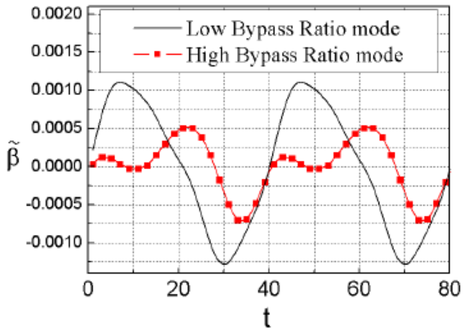

Figure 15. Exit angle disturbance at stator outlet

The unsteady wake has an important affect on the rotors downstream, so the wake transmission is also presented in Fig. 16 to compare the different loss mechanisms in two modes which can be thought of as a supplement of the causes of different efficiencies as well.

The wake suffers from being bent, cut and stretched in succession due to the axial and tangential pressure differential, velocity gradient and mixing of mainstream and wake. The results exhibit remarkable differences in the level of high entropy intensity and depth of the wake impact in two modes.

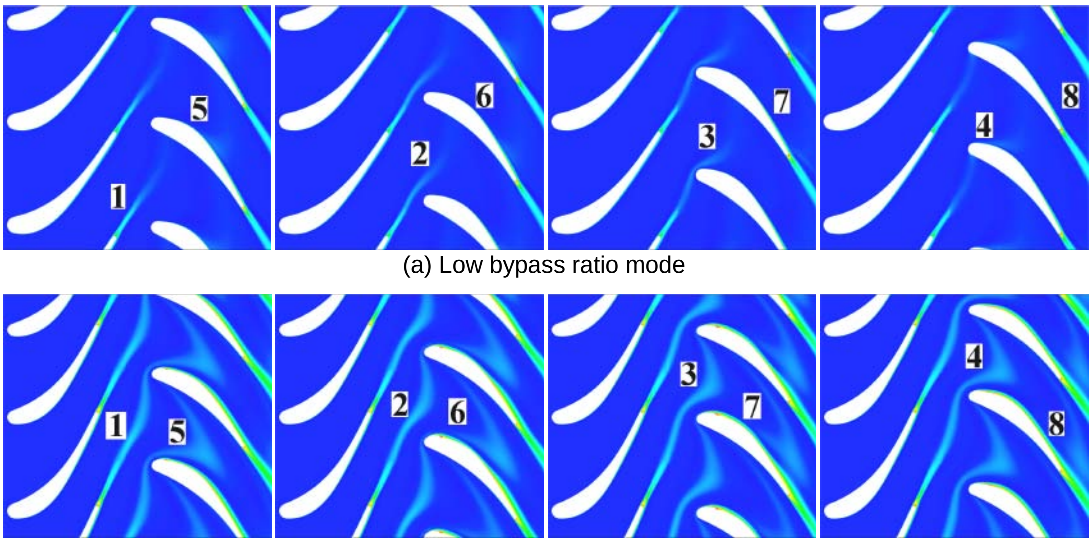

(a) Low bypass ratio mode

(b) High bypass ratio mode

Figure.16 Entropy-contours at mid-span

The brighter contours correspond to high entropy values, and the dark contours represent low values. A series of time numbers are printed on the pictures to make it easier to observe the transmission process. The wake suggested as number 1 in high bypass ratio mode has extended to the rotor passage above with the pressure side part of the wake produced by the neighbor stator, while it's lower and more independent in the low bypass ratio mode. The wake with high entropy is more obvious in the high bypass ratio mode which is presented next to explain the transport mechanism. When it enters the rotor passage as number 2, the near-wall region slows down due to viscosity while the mid-pitch region flows fast which makes the wake curved. Because of the pressure differential between the suction side and pressure side, the wake moves to the pressure side with low energy flows as the wake was transported downstream. Then it is cut by the leading edge into two regions shown as number 5 to 6. At the same time, the wake is stretched with increasing velocity and mixes with the mainstream slowly. On the suction surface, the low energy flows caused by separation is transported downstream to strengthen the rotor wake. Finally, two wake regions are shown at the rotor outlet. But in the low bypass ratio mode, the stator wake lasts only for about half axial chord before it mixes with the mainstream almost completely and the rotor wake is much lower.

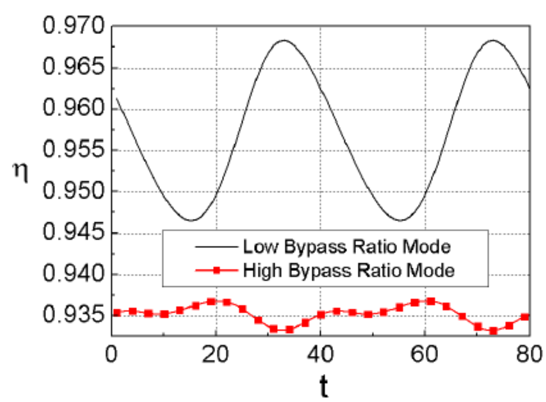

Figure.17 Unsteady efficiency

The phenomenon above reveals that the loss in high bypass ratio mode is more complicated and stronger, which aggravates stronger pressure fluctuation and lower efficiency. But the stagnant efficiency plotted as function of time in two modes shown in Fig.17 indicates that the turbine performs more gentle in high bypass ratio mode, and it reveals that the potential flow is the main factor for the whole flow field efficiency fluctuation while the local phenomena such as separation, shock wave and wake produce a relatively smaller interaction on it. The stator/rotor spacing may be the key reason for the unsteady potential flow [13].

CONCLUSIONS

A design method of VANT for VCE is presented in this article. Steady simulation is applied to acquire a series of turbine characteristic maps under many working conditions with two different vane stagger angles to verify its feasibility. It's shown in the efficiency map that the change of efficiency is selectivity that expansion ratio is the main factor at big stagger angle while relative speed plays a more important role at small stagger angle. The flow rate characteristics verify that it's effective to control the flow rate of the stage by changing the stator's stagger angle. The results of characteristics show that the turbine designed by the present method has satisfied the demands of efficiency, flow capacity and power capacity in two objective conditions, and it performs better with the stagger angle in low bypass ratio mode.

The steady flows under two objective conditions in two modes are analyzed to study the different efficiencies. As the reaction decreases, the stator performs better in the diffuser with less deceleration occurring in low bypass ratio mode, while a longer expansion region exits in high bypass ratio mode. Because of the radial pressure differential and wake, the flows in high bypass ratio mode at the stator outlet are uneven and the total pressure loss is 1.25% higher. The distribution of exit angle of stator depends on the stagger angle so as to influence the attack angle of the rotor downstream. Separation and shock are found at the mid-span of the rotor in high bypass ratio mode and they are more obvious at the hub. The decreased reaction and large attack angle are the main cause for different losses in the rotors of two modes.

The unsteady wake transmission reveals the different loss transport mechanism and supplements the reasons for different efficiencies in two modes. From the unsteady results, it can be concluded that the unsteady wake and secondary flows of stator are the main causes for higher rotor pressure fluctuation, while the potential flow plays an important role in efficiency fluctuation of the whole flow fields.

Acknowledgement

The authors sincerely thank Professor Zhu Zhili and all the members of turbine group of Beihang University for their support, encouragement, constructive suggestions and assistance.

Nomenclature

Cp	pressure coefficient
D	characteristic length
$G, \bar{G}$	massflow and reduced massflow
$\bar{G}_{max}$	choked reduced flow of the turbine in low bypass ratio mode
H	height of the blade
i	time
$L, \bar{L}$	power and reduced power
$\bar{L}_{max}$	reduced power corresponding to choked flow of the turbine in low bypass ratio mode
$n, \bar{n}$	wheel speed and reduced wheel speed
P	local static pressure
$\bar{P}$	time average static pressure
$\tilde{P}$	pressure disturbance
P_{in}^*	stagnant pressure at the inlet
T_{in}^*	stagnant temperature at the inlet
u_{in}	axial velocity at the inlet
ρ_{in}	density at the inlet
β	exit angle
$\bar{\beta}$	time average exit angle
$\tilde{\beta}$	exit angle disturbance
η	stagnant or overall efficiency
ξ	total pressure loss coefficient
π	expansion ratio
μ	viscosity coefficient

References

[1] Willis, E. A., Welliver, A. D.. "Variable-Cycle Engines for Supersonic Cruising Aircraft". AAIA/SAE 12th Propulsion Conference. 1976.

[2] Fang Changde. "Variable Cycle Engines". Gas Turbine Experiment and Research. 2008, 17 (3):1-6

[3] Thomas P. Moffitt etc. "Performance of a Single-Stage Turbine as Affected by Variable Stator Area". AIAAPPNO, 69-525, 1969.

[4] French, M. W., Allen, G. L.. "NASA VCE test bed engine aerodynamic performance characteristics and results". AIAA-81-1594.

[5] Fang Xiangjun, Liu Siyong etc. "Application of a 3D Blade Design Method for Supersonic Vaneless Contra-rotating Turbine". ASME GT 2008-50510, 2008

[6] Fang Xiangjun and Liu Siyong etc. The Basic Aerodynamic Design Study of Axial Transonic Highly Loaded Contra-rotating Turbine. Journal of Beijing University of Aeronautics and Astronautics, 2003, 29(6):475-479

[7] Reinmoller, U., Stephan, B., Schmidt, S., Niehuis, R.. "Clocking Effects in a 1.5 Stage Axial Turbine—Steady and Unsteady Experimental Investigations Supported by Numerical Simulations". ASME Journal of Turbomachinery, Vol. 124. 2002.1

[8] Ryan M. Urbassik, J. Mitch Wolff. "Unsteady aerodynamics and interactions between a high-pressure turbine vane and rotor". ASME Journal of Turbomachinery, Vol. 128. 2006.1

[9] Rai, M.M.. "Three-Dimensional Navier-Stokes Simulations of Turbine Rotor-Stator Interaction; Part I - Methodology and Part II – Results". Journal of Propulsion, Vol. 5, No. 3. 1989

[10] Liu Zhigang etc. "Design and analysis of hp-turbine for variable cycle engine". ASME GT 2010-22449, 2010.

[11] Qi Mingxu, Feng Zhenping. "Influence of Rotor-stator Interaction on The Performance of Axial-flow Turbine

Stages". Journal of Engineering Thermophysics. Vol. 24, No 1. 2003.1

[12] Jameson, A.. "Time dependent calculations using multigrid with applications to unsteady flows past airfoils and wings". AIAA 91-1596, 1991

[13] Haldeman, C. W., Krumanaker, M. L., Dunn, M. G.. "Influence of Clocking and Vane/Blade Spacing on the Unsteady Surface Pressure Loading for a Modern Stage and One-Half Transonic Turbine". ASME Journal of Turbomachinery, Vol. 125. 2003.10

